

Supplementary Information

Effects of hydrodynamic film boundary conditions on bubble-wall impact

Rogério Manica^a, Maurice Hendrix^b, Raghvendra Gupta^a,

Evert Klaseboer^a, Claus-Dieter Ohl^c and Derek Y.C. Chan^{ade}

^a *Institute of High Performance Computing, 1 Fusionopolis Way, Singapore 138632*

^b *Physics of Fluids, University of Twente, P.O. Box 217, 7500 AE Enschede, The Netherlands*

^c *School of Physical and Mathematical Sciences, Nanyang Technological University, Singapore 637371*

^d *Department of Mathematics and Statistics, University of Melbourne, Parkville 3010, Australia*

^e *Faculty of Life and Social Science, Swinburne University of Technology, Hawthorn 3122, Australia*

Description of the movie files

The videos show side-by-side images of the simultaneous recording of bubble rise from the side (right) and interferometric fringes from the top (left). These videos were analysed to produce the results of Figures 1 and 2 in the main manuscript.

Mobile and immobile hydrodynamic boundary conditions

To test the thin film boundary condition, we perform simulations for mobile and immobile air-water interface during drainage. In Fig. S1 we show that our film drainage data can be best modelled using the tangentially mobile boundary condition at the air-water interface. We have simulated an immobile boundary for both cases presented in the main text. Though the main features are still there, the immobile boundary condition results are considerably different compared to the experiment. If the boundary condition would have been immobile, the hydrodynamic pressure would have risen quickly and the film would have dimpled at a larger separation compared to the mobile and experiment. Also, the mobile boundary condition would provide a rupture time that is shorter compared to the immobile case. For the numerical results the film is much thicker at time $t = 100$ s for the immobile bubble and adhesion would not happen. On the other hand, the mobile simulations predict the film to be about 100 nm, and adhesion is about to occur.

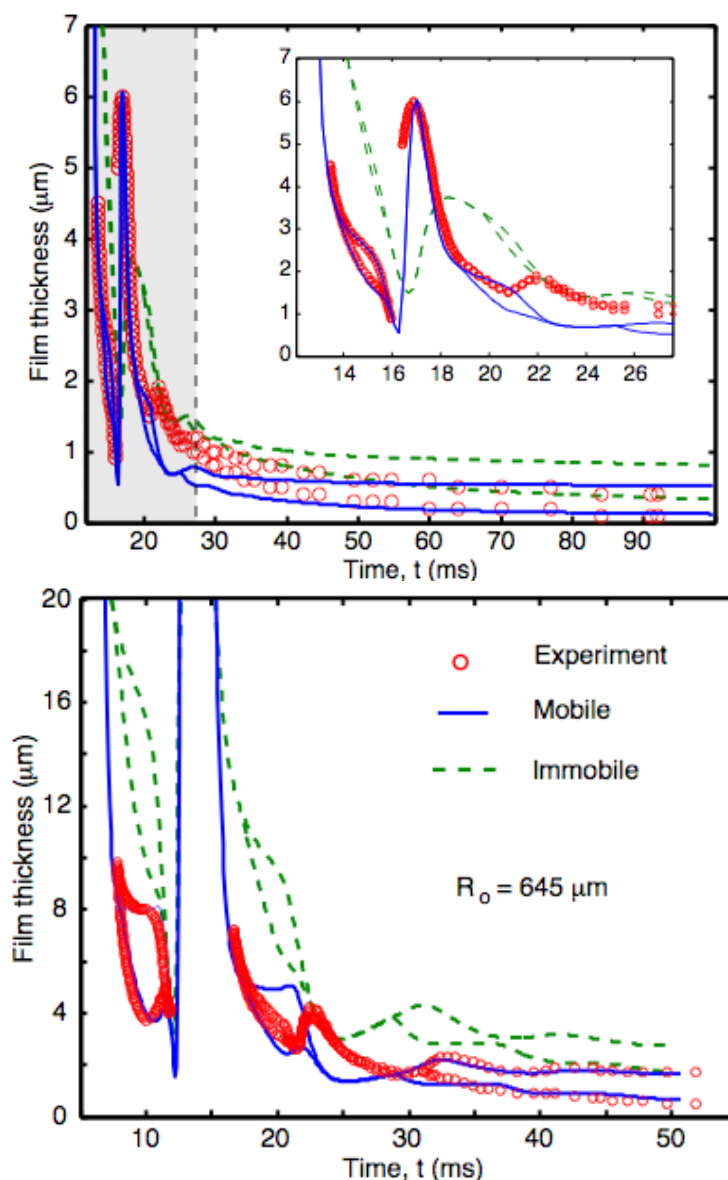


Figure S1. Comparison between experiment and theory: Circles represent experimental values determined from interference fringes and lines are predictions from lubrication theory using the tangentially mobile (full line) and immobile (dashed line) boundary condition at the bubble-water interface.

Drag coefficient and numerical implementation

We solve the Navier-Stokes equations numerically in axially symmetric form using ANSYS Fluent to capture the drag coefficient under mobile, immobile and stagnant cap boundary conditions at the air-water interface for a rigid sphere. By stagnant cap we mean that part of the bubble surface at the top is mobile while the remaining of the surface presents immobile boundary condition due to coverage of that part of the bubble

by surface-active materials. We assume deformation is negligible and thus the bubble remains spherical, a reasonable assumption considering that the Weber number of our system is smaller than unity. The drag coefficients for Reynolds numbers 100 and 200, in the range of our experimental data, are calculated and plotted in Fig. S2.

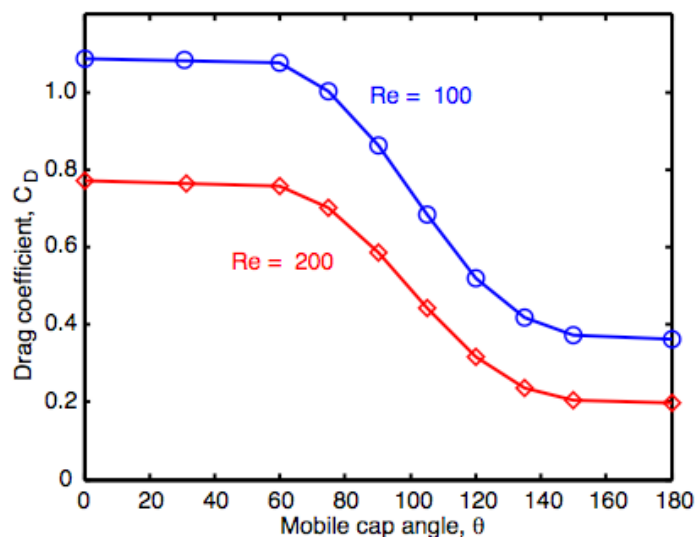


Figure S2. Drag coefficient calculations using ANSYS Fluent simulations for different mobile cap angles for $Re = 100$ and 200 .